New strategy for registering DW and non-DW images via tensor estimation metric

C. Koay[1,2], A. L. Alexander[1], and M. E. Meyerand[1]
[1]Department of Medical Physics, University of Wisconsin-Madison, Madison, WI, United States, [2]STBB, National Institutes of Health, Bethesda, MD, United States

INTRODUCTION Registration of DW and non-DW images is a critical step within the whole DTI data-processing pipeline. Even in non-clinical setting, the importance of a robust and accurate image registration cannot be underestimated. This is due to the fact that eddy current will still have an effect on DW image quality even when there is no subject-motion or physiological noise; this is particularly true in high b-value or q-value diffusion imaging. While there are currently two highly promising image-registration methods for DTI [1-2], the former does not provide the goodness-of-fit of DW images to the T_2-weighted image and the latter is generic method based on mutual information, which makes the assessment of goodness-of-registration between DW and nonDW images more complicated. In this study, we proposed a simple DW and non-DW image registration strategy that provides the much needed information on the goodness-of-registration of DWI images to the T_2-weighted image within the registration process. The key idea of this proposal is built upon the work of [3] and it uses DW images to estimate the T_2-image. This strategy requires very minimal modification to the existing acquisition of DTI or the estimation procedures [3].

METHODS For each diffusion weighted image, we have $S_i = S_0 \exp(-b_i(\mathbf{g}^i)^T \cdot \mathbf{D} \cdot \mathbf{g}^i)$, with $i = 1,\ldots,N$ or $\mathbf{y} = \mathbf{W}\boldsymbol{\gamma}$ in matrix form, where $\mathbf{y} = [\ln(S_1) \quad \cdots \quad \ln(S_N)]^T$, $\boldsymbol{\gamma} = [\ln S_0 \quad D_{xx} \quad D_{yy} \quad D_{zz} \quad D_{xy} \quad D_{yz} \quad D_{xz}]^T$, and $\mathbf{W}$ is matrix whose components are functions of the diffusion weightings b_i and components of the unit gradient direction vectors. The notation is kept consistent with that of [3]. Two-stage weighted least squares method is used for the registration between the DWI and the T_2-weighted images by first transforming all the DW images and then evaluating the goodness-of-fit of the weighted linear least squares (WLLS) estimation to the tensor. The cost function is modeled as a combination between the residual sum of squares of the spatially transformed version of $\mathbf{y}$, denoted by $\tilde{\mathbf{y}}$ with the attempt to match the DW images to $\ln S_0$, which is define throughout the region of interest. Therefore, the objective function is $\sum \left\{ \left\| \tilde{\mathbf{y}} - \hat{\mathbf{y}} \right\|^2 + (\ln S_0 - \ln \hat{S}_0)^2 \right\}$ where the summation is done within the region of interest. Note that $\hat{\mathbf{y}}$ and $\hat{S}_0$ are the estimated values from the WLLS and S_0 is the T_2-weighted signal from the target image. Further note that the design matrix, $\mathbf{W}$, does not have to include b= 0 sec/ mm^2 but it does require at least two different b-values to be non-singular. The geometric transformation used in this study on the DWI images was the 2D-affine transformation (7 parameters for each DWI image) with bilinear interpolation. A mask was created to include the region of interest (the ROI is the whole brain for this study).

RESULTS The set of encoding directions used in this experiment has twelve directions. The width, spacing, and amplitude of the diffusion gradient pulses for the b_1 were 25 msec, 36 msec, and 30 mT/m, respectively. This yielded b_1=1113.91 sec/ mm^2. As for the b_2, the gradient amplitude was set to 13 mT/m and this yielded b_2=209.18 sec/ mm^2. Other imaging parameters were TR = 4.68 sec, TE = 79.5 msec, field-of-view (FOV) = 240 × 240 mm^2, slice thickness = 4mm, and 3 NEX for averaging. Figure 1 (A) and Fig 1(B) are the error maps. Figure 1(C) is the histogram of these maps and Fig 1(D) shows the tails of these histograms. Relevant information and descriptive statistics about these data are summarized in Fig 1(E).

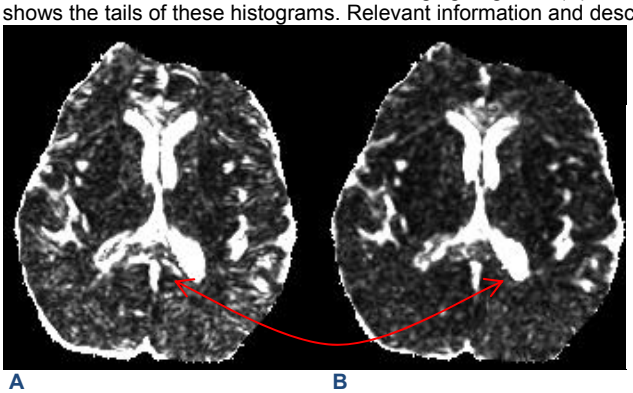

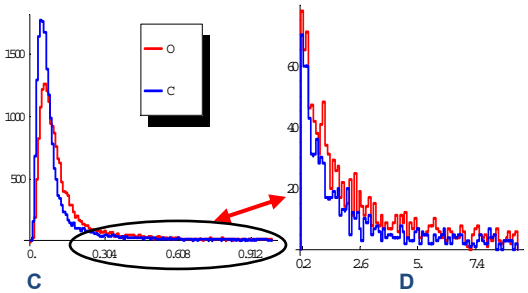

O = original data
C = corrected data
Sample Size (ROI): 20064

	O	C
Mean	0.5698	0.2929
Std.	2.1270	1.0259

A B C D E

FIG 1.(A) The error maps before correction and (B) after correction, both images are set with common min and max values. (C) The histograms of the maps, the histogram of the uncorrected data is in red and the histogram of the corrected data is in blue. (D) The tails of the histograms. (E) The basic information and descriptive statistics about these two data.

DISCUSSION The proposed method is an important step toward a more practical means of evaluating not only the goodness-of-registration among DW images, as was the case with [1], but also with some gold standard or template, which may be T_2-weighted images, in a consistent manner. This approach can accommodate multiple b-values and requires at least two non-zero and distinct b-values. Our approach is different from that of [1] in two important ways. First, the formulation proposed by [1] is restricted to a single b-value while ours can accommodate multiple b-values; however, it requires at least two distinct b-values. Second, our objective function is novel in the context of DW and non-DW image registration and is based upon estimates derived from the WLLS rather than unweighted or ordinary linear least squares (LLS), which was the case with [1]. LLS has been shown in simulation [6] and in theoretical analysis [3] to be suboptimal. Figure 1(A) and figure 1(B) are the error maps before and after correction. Each pixel value is the value of the term in the above mentioned summation evaluated at that location. The reduction of error is substantial in white matter regions. Figure 1(C) and Figure 1(D) are the histograms of the error map data. From Fig 1(E), it can be shown that the difference between these two data is significant and the reduction in error is about 48.6%. We also found that negative eigenvalues [5,4] in white matter region near the interface between Corpus Callosum and the ventricle were reduced in number after registration.

REFERENCES [1]. Andersson et al. NeuroImage 2002; 16, 177-199. [2]. Rodhe et al. Magn Reson Med 2004;51:103-114. [3]. Koay et al. Journ. Magn. Reson 2006; 182: 115-125. [4]. Koay et al. Magn Reson Med 2006; 55:930–936. [5]. Wang et al. IEEE Trans Med Imaging 2004;23:930–939. [6] Jones et al. Magn. Reson. Med. 52 (2004) 979–993.